Dual control of RegX3 transcriptional activity by SenX3 and PknB

Received for publication, February 27, 2019, and in revised form, May 30, 2019 Published, Papers in Press, June 3, 2019, DOI 10.1074/jbc.RA119.008232

Eun-Jin Park[‡], Yu-Mi Kwon[§¶], Jin-Won Lee[¶], Ho-Young Kang[‡], and Jeong-Il Oh[‡1]

From the [‡]Department of Microbiology, Pusan National University, Busan 46241, Republic of Korea, the [§]Biomedical Research Institute, Center for Theragnosis, Korea Institute of Science and Technology, Seoul 02792, Republic of Korea, and the [¶]Department of Life Science and Research Institute for Natural Sciences, Hanyang University, Seoul 04763, Republic of Korea

Edited by Chris Whitfield

The mycobacterial SenX3–RegX3 two-component system consists of the SenX3 sensor histidine kinase and its cognate RegX3 response regulator. This system is a phosphorelay-based regulatory system involved in sensing environmental P_i levels and induction of genes required for P_i acquisition under P_i-limiting conditions. Here we demonstrate that overexpression of the kinase domain of *Mycobacterium tuberculosis* PknB (PknB-KD^{Mtb}) inhibits the transcriptional activity of RegX3 of both *M. tuberculosis* and *Mycobacterium smegmatis* (RegX3^{Mtb} and RegX3^{Ms}, respectively). Mass spectrometry results, along with those of *in vitro* phosphorylation and complementation analyses, revealed that PknB kinase activity inhibits the transcriptional activity of RegX3^{Mtb} through phosphorylation events at Thr-100, Thr-191, and Thr-217. Electrophoretic mobility shift assays disclosed that phosphorylation of Thr-191 and Thr-217 abolishes the DNA-binding ability of RegX3^{Mtb} and that Thr-100 phosphorylation likely prevents RegX3^{Mtb} from being activated through conformational changes induced by SenX3-mediated phosphorylation. We propose that the convergence of the PknB and SenX3-RegX3 signaling pathways might enable mycobacteria to integrate environmental P_i signals with the cellular replication state to adjust gene expression in response to P_i availability.

The adaptation and survival of *Mycobacterium tuberculosis* (*Mtb*)[2] under hostile host environments require exquisite regulation of gene expression in response to changing environments (1, 2). Phosphorelay through proteins is a major mechanism by which environmental signals are transmitted to elicit appropriate adaptive responses (3, 4). Two-component systems (TCSs), which constitute the primary regulatory systems utilizing phosphorelay in prokaryotes, consist of sensory histidine kinases (HKs) and their cognate response regulators (RRs). In response to a specific ligand or environmental signal, an HK is autophosphorylated on a conserved histidine residue. The phosphoryl group is subsequently transferred from the HK to an aspartate residue conserved in the N-terminal receiver domain of the partner RR to activate the RR effector domain. Because most RRs contain the helix–turn–helix DNA-binding motif as an effector domain, the activated RRs normally serve as active transcription factors to regulate gene expression (5–10). *Mtb* possesses 11 paired TCSs and five orphan RRs (11–13). Of 11 paired TCSs, the SenX3-RegX3 TCS has been suggested to play an important role mainly in the adaptation of mycobacteria to P_i-limiting conditions (14, 15). Other roles have also been suggested with regard to virulence (16–19), persister formation (20), sensing of diatomic gases (O_2, NO, and CO) (21), and membrane vesicle biogenesis (22). When the level of P_i falls below a certain threshold value in the environment, the SenX3 HK is activated to phosphorylate the RegX3 RR. The activated RegX3 RR positively regulates expression of many genes, including those implicated in the acquisition of P_i under P_i-limiting conditions, such as the *pstSCAB* operon encoding a high-affinity phosphate-specific ABC transporter (Pst) and the *phoA* gene encoding alkaline phosphatase (14, 23, 24). Although the mechanism by which the SenX3 HK senses P_i availability has not yet been fully elucidated, SenX3 appears not to sense P_i levels by itself. The kinase/phosphatase activity of SenX3 has been suggested to be regulated by the functional state of the Pst uptake system with the assistance of other auxiliary proteins (PhoU in *Mycobacterium smegmatis* and PhoY in *Mtb*). This suggestion was made on the basis of the finding that inactivation of either Pst transporter or PhoU (PhoY) by mutation brings about constitutive activation of the SenX3–RegX3 TCS and constitutive expression of the RegX3 regulon independent of P_i availability (20, 24, 25). According to the suggested model, the Pst transporter generates an inhibitory signal under P_i-replete conditions that is transmitted by PhoU (PhoY) to the SenX3 HK. The inhibitory signal shifts the equilibrium of SenX3 activity from the kinase mode to the phosphatase mode, resulting in repression of the RegX3 regulon. The PhoU and PhoY proteins have been suggested to function as adaptor proteins between the Pst transporter and SenX3 through their interactions between the Per–ARNT–Sim (PAS) domain of SenX3 and the PstB ATPase subunit of the Pst system (26–28).

This work was supported by the Basic Science Research Program through the National Research Foundation of Korea funded by the Ministry of Education, Science, and Technology (NRF-2014R1A2A1A11051572). The authors declare that they have no conflicts of interest with the contents of this article.

This article contains Figs. S1–S7, Tables S1 and S2, and supporting experimental procedures.

[1] To whom correspondence should be addressed. Tel.: 82-51-510-2593; Fax: 82-51-514-1778; E-mail: joh@pusan.ac.kr.

[2] The abbreviations used are: *Mtb*, *Mycobacterium tuberculosis*; TCS, two-component system; HK, histidine kinase; RR, response regulator; PAS, Per–ARNT–Sim; STPK, Ser/Thr protein kinase; KD, kinase domain; Y2H, yeast two-hybrid; qPCR, quantitative PCR; IPTG, isopropyl 1-thio-β-D-galactopyranoside; PASTA, protein and Ser/Thr kinase–associated; SD, synthetic defined dropout; CBB, Coomassie Brilliant Blue.

Under P_i-limiting conditions, the inhibitory signal is diminished or removed, which renders SenX3 active to phosphorylate the RegX3 RR. Intriguingly, a recent study demonstrated that the SenX3 HK is a hemoprotein with a *b*-type heme accommodated in its PAS domain and that oxidation of the heme from a ferrous to a ferric state enhances SenX3 autokinase activity, whereas binding of NO or CO to the heme leads to inhibition of autokinase activity (21). This finding suggests the possibility that SenX3 can also serve as a sensor kinase for diatomic gases such as O_2, NO, and CO.

Because a eukaryotic-like Ser/Thr protein kinase (STPK) was first characterized in *Myxococcus xanthus* (29), many STPKs have been identified and characterized in bacteria, and increasing attention has been paid to the importance of STPKs in prokaryotic signaling pathways related to stress responses, development, virulence, regulation of central metabolism, as well as cell division and morphology (30–33). In contrast to HKs that have a strict substrate specificity, STPKs can normally phosphorylate multiple substrates, resulting in pleiotropic responses from a single signal in the signal transduction pathway (31). The genomes of *Mtb* and *M. smegmatis* contain 11 and 13 STPK genes, respectively (11, 34). The membrane-bound PknB is one of 11 STPKs in *Mtb* and is conserved in all mycobacteria (34). It has been shown to be essential for both *Mtb* and *M. smegmatis* (35–37) and to be involved in cell elongation, division, peptidoglycan biosynthesis, and regulation of oxygen-dependent cell replication (38–40).

Cross-talk between STPKs and TCSs have been reported to take place in several bacterial regulatory systems (41–50). Recently, we demonstrated that the purified kinase domain of *Mtb* PknB (PknB-KD^{Mtb}) robustly phosphorylated six RRs (RegX3, NarL, KdpE, TrcR, DosR/DevR, and MtrA) among 11 paired RRs of *Mtb* and that overexpression of PknB-KD^{Mtb} in *M. smegmatis* led to significant inhibition of DosR (DevR) transcriptional activity by phosphorylating Thr-180 located in the helix–turn– helix motif of DosR (DevR) (50). As an extension of our previous study, here we report that overexpression of PknB-KD^{Mtb} significantly inhibits the transcriptional activity of RegX3 of *Mtb* (RegX3^{Mtb}) by phosphorylating Thr-100, Thr-191, and Thr-217.

Results

Protein–protein interactions between RegX3 and PknB

We demonstrated previously that purified RegX3^{Mtb} was strongly phosphorylated by purified PknB-KD^{Mtb} *in vitro* (50). Because phosphorylation of RegX3^{Mtb} by PknB^{Mtb} seems to require protein–protein interactions between them, we determined protein interactions between RegX3^{Mtb} and PknB^{Mtb} by yeast two-hybrid (Y2H) assay. PknE (one of 11 STPKs in *Mtb*) and SenX3 of *Mtb* (SenX3^{Mtb}) were included in the experiment as negative and positive controls, respectively (Fig. 1). For the Y2H assay, the *regX3*^{Mtb} gene was cloned into the prey vector pGADT7linker, whereas the gene portions encoding the KDs of PknB^{Mtb}, PknE^{Mtb}, and SenX3^{Mtb} were cloned into the bait vector pGBKT7. Consistent with a previous report (51), the yeast strain coexpressing RegX3^{Mtb} and SenX3^{Mtb} grew well in the absence of histidine (−His), indicating protein–protein interactions between RegX3^{Mtb} and its cognate SenX3^{Mtb} HK. Coexpression of PknB^{Mtb} with RegX3^{Mtb} led to growth of yeast in the absence of histidine whereas coexpression of PknE^{Mtb} with RegX3^{Mtb} did not. As expected, the yeast strains expressing either SenX3^{Mtb} or PknB^{Mtb} alone without expression of RegX3^{Mtb} did not grow on −His medium. Taken together, the Y2H results suggest a possible interaction of RegX3^{Mtb} with PknB^{Mtb}.

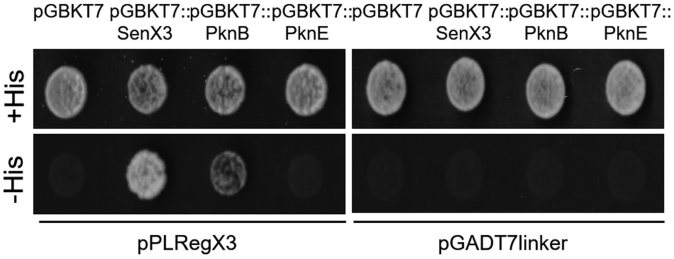

Figure 1. Determination of protein–protein interactions between RegX3^{Mtb} and PknB^{Mtb} in the Y2H assay. The *regX3*^{Mtb} gene was cloned into the pGADT7 linker (encoding the GAL4 activation domain), resulting in pPLRegX3. The gene portions encoding the KDs of *Mtb* PknB, PknE, and SenX3 were cloned into pGBKT7 (encoding the GAL4 DNA-binding domain). Yeast strains cotransformed with both pPLRegX3 and pGBKT7 derivatives were used for the Y2H assay. To distinguish false positive interactions, the empty pGADT7linker vector was introduced into the yeast strains containing the pGBKT7 derivatives in place of pPLRegX3, and the resulting yeast strains were used as negative controls. All yeast strains were spotted onto SD/−Leu/−Trp plates (+*His*) and histidine-deficient SD/−Leu/−Trp/−His plates (−*His*).

Overexpression of PknB-KD^{Mtb} inhibits RegX3 transcriptional activity in vivo

To assess the effect of RegX3 phosphorylation by PknB on the transcriptional activity of RegX3, we overexpressed PknB-KD^{Mtb} in *M. smegmatis* and examined the transcriptional activity of RegX3 by determining the expression level of the *phoA* gene, which encodes alkaline phosphatase and is regulated by the SenX3–RegX3 TCS. Because RegX3^{Ms} (MSMEG_0937) shares 93% identity with RegX3^{Mtb} at the amino acid level (Fig. S1), we employed *M. smegmatis* overexpressing PknB-KD^{Mtb} in place of *Mtb* to examine the overexpression effect of PknB-KD^{Mtb} on RegX3 transcriptional activity. The gene portion encoding PknB-KD^{Mtb} was overexpressed from an acetamide-inducible promoter on pMHPknB that is a derivative of the pMH201 integration vector. Before determining the effect of PknB-KD^{Mtb} overexpression on the transcriptional activity of RegX3, we examined the overexpression effects of PknB-KD^{Mtb} on aerobic growth of *M. smegmatis* under P_i-replete and P_i-limiting conditions (Fig. S2). The *M. smegmatis* control strain with pMH201 grew under P_i-replete conditions approximately three times faster than the same strain under P_i-limiting conditions. Although growth of the *M. smegmatis* strain was severely inhibited by PknB-KD^{Mtb} expressed from pMHPknB under both P_i-replete and P_i-limiting conditions, the optical density at 600 nm (A_{600}) and colony-forming unit values of the cultures of the *M. smegmatis* strain with pMHPknB were increased over time, indicating that overexpression of PknB-KD^{Mtb} is not lethal to *M. smegmatis* but significantly inhibits its growth under conditions tested in this study. The expression level of *phoA* in *M. smegmatis* was determined using a *phoA*::*lacZ* transcriptional fusion plasmid, pNCphoA. As shown in Fig. 2*A*, *phoA*

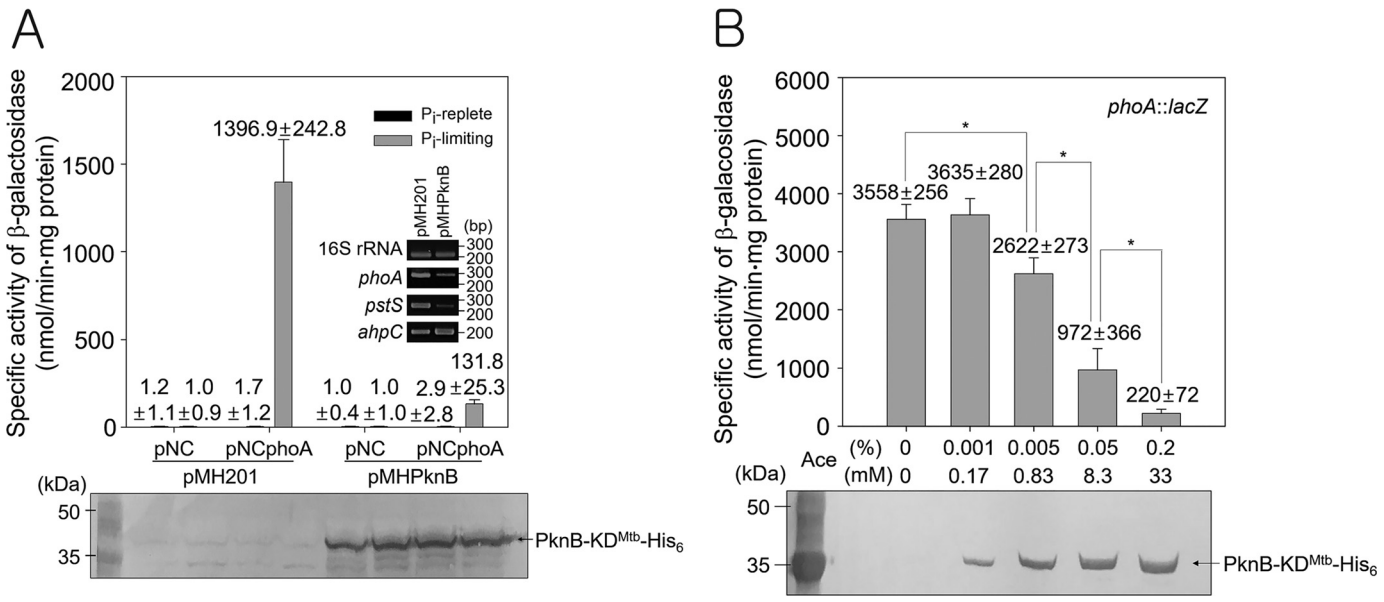

Figure 2. Effect of PknB-KD^{Mtb} overexpression on *phoA* expression in *M. smegmatis*. *A*, pMH201-derived pMHPknB was employed for overexpression of PknB-KD^{Mtb} in *M. smegmatis*. The overexpression effect of PknB-KD^{Mtb} on RegX3 transcriptional activity was examined by determining the expression level of *phoA* in *M. smegmatis* strains harboring an *phoA*::*lacZ* transcriptional fusion plasmid (pNCphoA) and pMHPknB. The expression level of *phoA* was measured by determining β-gal activity in the *M. smegmatis* strains. As controls, the *M. smegmatis* strain with both pNCphoA and pMH201 as well as the *M. smegmatis* strains harboring pNC in place of pNCphoA were included in the experiment. The *M. smegmatis* strains were grown aerobically to an A_{600} of 0.4–0.5 in glucose–MOPS medium under P_i-replete or P_i-limiting conditions in the presence of 0.2% (w/v) of acetamide. The expression levels of *phoA*, *pstS*, and *ahpC* in the WT strains of *M. smegmatis* containing pMHPknB or pMH201 were also determined by RT-PCR. RT-PCR of the 16S rRNA gene was performed to ensure that same amounts of total RNA were used for RT-PCR. *B*, the expression level of *phoA* was measured by determining β-gal activity in the *M. smegmatis* strains with pMHPknB and pNCphoA. The *M. smegmatis* strains were grown aerobically to an A_{600} of 0.4–0.5 in glucose–MOPS medium under P_i-limiting conditions in the presence of increasing concentrations of acetamide (*Ace*) ranging from 0.001 to 0.2% (w/v). The same strain cultured in the absence of acetamide was included as a control. All values are the averages of the results from either three (*A*) or five (*B*) independent determinations, respectively. The *error bars* indicate standard deviations. Western blot analysis was performed for detection of the expressed His_6-tagged PknB-KD^{Mtb}. Cell-free crude extracts (either 20 μg (*A*) or 30 μg (*B*)) were separated on SDS-PAGE, followed by Western blot analysis with a His tag antibody. *, $p < 0.01$.

expression was strongly induced in the *M. smegmatis* strain with both pNCphoA and pMH201 grown under P_i-limiting conditions compared with the same strain grown under P_i-replete conditions. However, the *M. smegmatis* strain harboring both pNCphoA and pMHPknB showed a significantly decreased level of *phoA* expression under P_i-limiting conditions relative to the control strain with pNCphoA and pMH201 grown under P_i-limiting conditions. As expected, virtually no β-gal activity was detected in the *M. smegmatis* strains with the pNC empty vector. The overexpression effect of PknB-KD^{Mtb} on expression of *phoA* was also examined at the transcript level by RT-PCR analysis (Fig. 2*A*, *inset*). We additionally determined the expression of *pstS* and *ahpC* in the RT-PCR analysis as controls. The *pstSCAB* operon is known to be under control of the SenX3–RegX3 TCS-like *phoA* (14), whereas the *ahpC* gene for alkyl hydroperoxide reductase is known to be regulated by FurA and Crp but not by RegX3 (52, 53). RT-PCR analysis revealed that expression of *phoA* and *pstS* was significantly inhibited by PknB-KD^{Mtb} overexpression. In contrast, overexpression of PknB-KD^{Mtb} resulted in a slight increase in *ahpC* expression, which is consistent with our previous observation (50). Overexpression of PknB-KD^{Mtb} in the *M. smegmatis* strain harboring pMHPknB was verified by Western blot analysis using a His tag antibody. Altogether, the results indicate that overexpression of PknB-KD^{Mtb} inhibits the transcriptional activity of RegX3^{Ms}. To determine whether *phoA* expression correlates with the expression level of PknB-KD^{Mtb}, the expression level of *phoA* was determined in the *M. smegmatis* strain with both pMHPknB and pNCphoA after it had been grown under P_i-limiting conditions with treatment of increasing concentrations of acetamide. As shown in Fig. 2*B*, the expression level of *phoA* was gradually reduced with increasing concentrations of acetamide used in cultures. Western blot analysis showed that the amount of expressed PknB-KD^{Mtb} was proportional to the concentration of treated acetamide. Taken together, the results indicate that the transcriptional activity of RegX3^{Ms} is inversely related to the expression extent of PknB-KD^{Mtb}. It has been suggested that PknB and PknH might serve as the top-tier master STPKs in the hierarchical STPK-signaling cascade of *Mtb* (54). We examined whether overexpression of PknH-KD^{Mtb} (amino acids 1–310) also inhibits *phoA* expression using an *M. smegmatis* strain overexpressing PknH-KD^{Mtb} (Fig. S3). It has been demonstrated previously by Western blot analysis that PknH-KD^{Mtb} is overexpressed in the *M. smegmatis* strain with pMHPknH grown in the presence of acetamide (50). When *M. smegmatis* strains were grown under P_i-limiting conditions in the presence of acetamide, the expression level of *phoA* was only marginally decreased in the *M. smegmatis* strain carrying pMHPknH relative to that in the *M. smegmatis* strain with pMH201. This result suggests that overexpression of PknH-KD^{Mtb} does not affect RegX3 transcriptional activity and that the observed inhibitory effect of *phoA* expression by PknB-KD^{Mtb} overexpression is at least to some extent specific to PknB.

We next examined whether overexpression of PknB-KD^{Mtb} also inhibits the transcriptional activity of RegX3^{Mtb} *in*

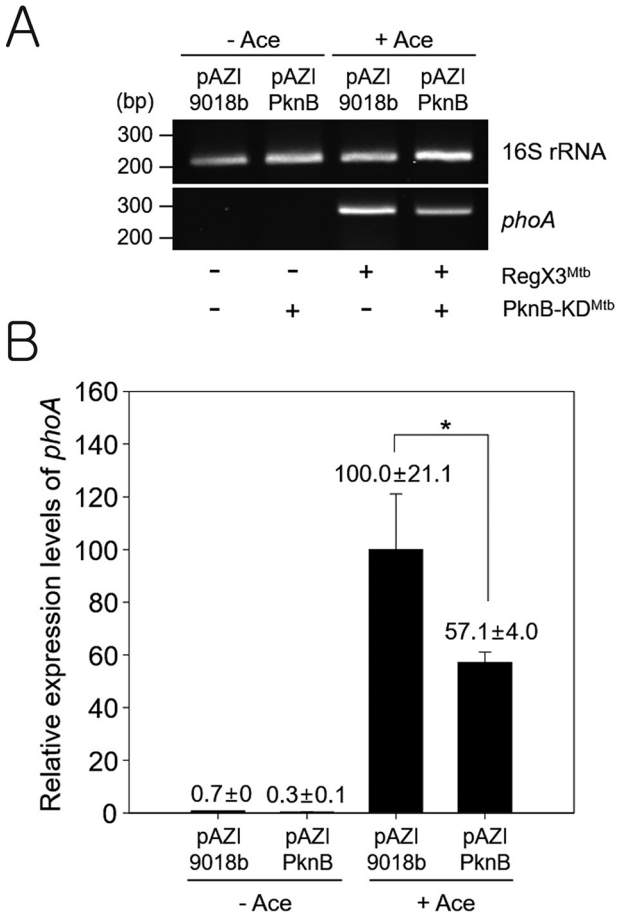

Figure 3. Inhibition of the transcriptional activity of RegX3^{Mtb} by PknB-KD^{Mtb} *in vivo*. *A* and *B*, the pAZI9018b-derived pAZIPknB, which was used for overexpression of PknB-KD^{Mtb}, carries the gene encoding PknB-KD^{Mtb}, which is under the control of an IPTG-inducible promoter. The Δ*regX3* conditional mutant strains of *M. smegmatis* harboring either pAZIPknB or pAZI9018b were aerobically grown to an A_{600} of 0.4–0.5 in glucose–MOPS medium containing 0.5 mM IPTG in the presence (+*Ace*) or absence (−*Ace*) of 0.2% (w/v) acetamide under P_i-limiting conditions. The expression level of *phoA* was determined by RT-PCR (*A*) and real-time qPCR (*B*). The level of mRNA specific for *phoA* determined by real-time qPCR was normalized to that of 16S rRNA. The level of *phoA* mRNA in the strain containing pAZI9018b grown in the presence of acetamide is set at 100, and the relative values are expressed for the other strains. All values are the means of the results from three independent determinations. The *error bars* indicate standard deviations. *, $p < 0.05$.

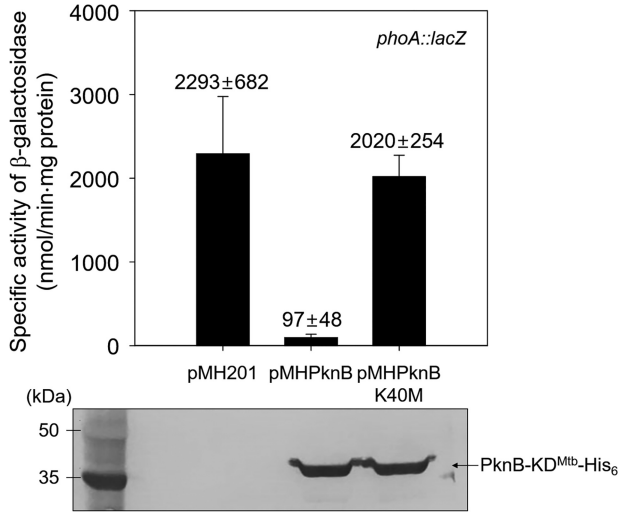

Figure 4. Overexpression effect of inactive PknB-KD^{Mtb} on *phoA* expression. The WT and K40M mutant forms of PknB-KD^{Mtb} were overexpressed from the pMH201 derivatives pMHPknB and pMHPknBK40M, respectively. The empty pMH201 vector and its derivatives were integrated into the chromosome of the *M. smegmatis* strain carrying pNCphoA. The promoter activity of *phoA* was measured by determining β-gal activity in the strains grown aerobically to an A_{600} of 0.4–0.5 under P_i-limiting conditions in the presence of 0.2% (w/v) acetamide. Crude extracts (30 μg) of the three strains were subjected to Western blot analysis with a His tag antibody to determine the amounts of expressed PknB-KD^{Mtb}.

vivo using a Δ*regX3* conditional mutant strain of *M. smegmatis.* The Δ*regX3* conditional mutant of *M. smegmatis* with deletion of its own *regX3*^{Ms} gene carries the acetamide-inducible *regX3*^{Mtb} gene on the chromosomal DNA. Therefore, the mutant was expected to exhibit mutant phenotypes in the absence of acetamide, whereas RegX3^{Mtb} was expected to be overexpressed in the mutant in the presence of acetamide. The transcriptional activity of RegX3^{Mtb} was examined by determining the expression level of *phoA* by RT-PCR and real-time qPCR (Fig. 3). Because the pAZI9018b-derived pAZIPknB, which was used for overexpression of PknB-KD^{Mtb}, carries the gene encoding PknB-KD^{Mtb} that is under the control of an IPTG-inducible promoter, addition of IPTG to the growth medium led to overexpression of PknB-KD^{Mtb}. When grown under P_i-limiting conditions in the presence of both IPTG and acetamide, the Δ*regX3* conditional mutant strain with pAZIPknB showed a 43% decrease in *phoA* expression relative to the mutant strain with the empty pAZI9018b vector grown under the same conditions. When grown under P_i-limiting conditions without acetamide, *phoA* expression was almost abolished in both the mutant strains because of the lack of RegX3^{Mtb} expression. In contrast to the strong inhibition (~90%) of RegX3^{Ms} transcriptional activity by overexpression of PknB-KD^{Mtb} in the WT strain of *M. smegmatis* (Fig. 2*A*), overexpression of PknB-KD^{Mtb} in the Δ*regX3* conditional mutant of *M. smegmatis* reduced the transcriptional activity of RegX3^{Mtb} to a lesser extent, which might be attributable to the overexpression effect of RegX3^{Mtb} in the Δ*regX3* conditional mutant strain grown in the presence of acetamide. Considering the results shown in Figs. 2 and 3, we suggest that the increased kinase activity of PknB^{Mtb} inhibits the transcriptional activity of both RegX3^{Mtb} and RegX3^{Ms}.

Inhibition of RegX3 transcriptional activity by PknB-KD^{Mtb} overexpression results from the kinase activity of PknB-KD^{Mtb}

It is conceivable that the inhibition of RegX3^{Ms} transcriptional activity in *M. smegmatis* by PknB-KD^{Mtb} overexpression is a consequence of the sequestration of RegX3^{Ms} by the overexpressed PknB-KD^{Mtb} through their protein–protein interactions rather than by increased PknB kinase activity. To examine this possibility, we determined the overexpression effect of inactive PknB-KD^{Mtb} with the K40M mutation (37, 38) on *phoA* expression in *M. smegmatis* (Fig. 4). The mutant form of PknB-KD^{Mtb} was overexpressed using pMHPknBK40M, which has the same construct as pMHPknB except for the K40M mutation in *pknB*. The transcriptional activity of RegX3^{Ms} was determined by measuring the promoter activity of *phoA* in *M. smegmatis* strains harboring pNCphoA. When grown under P_i-limiting conditions, the *M. smegmatis* strain with both pMH201 and pNCphoA exhibited a high expression level of

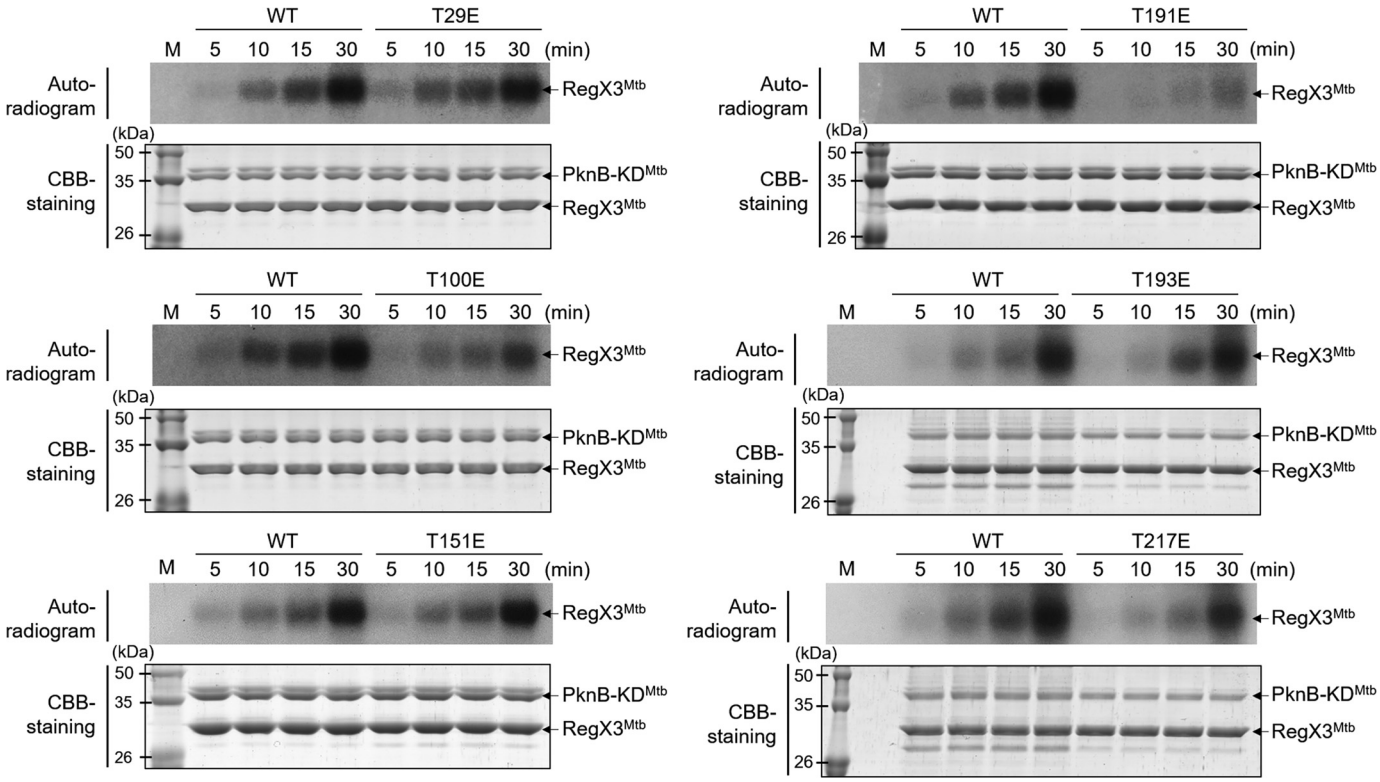

Figure 5. Effect of T29E, T100E, T151E, T191E, T193E, and T217E mutations on phosphorylation of RegX3^{Mtb} by PknB-KD^{Mtb}. 0.05 nmol of PknB-KD^{Mtb} was mixed with 0.1 nmol of the WT and mutant forms (T29E, T100E, T151E, T191E, T193E, and T217E) of RegX3^{Mtb} in 20 μl of reaction buffer (20 mM Tris-Cl (pH 7.5), 50 mM NaCl, 10 mM $MgCl_2$, and 10 mM $MnCl_2$). The phosphorylation reactions were started by adding 100 μM cold ATP and 1,000 Ci/mole [γ-^{32}P]ATP, incubated at 30 °C, and terminated at the indicated time points. Thereafter, proteins were resolved by SDS-PAGE. Phosphorylated RegX3^{Mtb} proteins were detected by autoradiography. The duplicated reaction mixtures without addition of ATP were subjected to SDS-PAGE, and the gels were stained by CBB. As loading controls, the stained gels are presented below the autoradiograms to compare the amounts of the purified WT and mutant forms of RegX3^{Mtb} used in the assay. *M,* molecular weight marker lanes.

phoA, whereas overexpression of PknB-KD^{Mtb} almost abolished *phoA* expression in the *M. smegmatis* strain with pMHPknB and pNCphoA, which is consistent with the result shown in Fig. 2*A*. However, overexpression of the K40M mutant form of PknB-KD^{Mtb} in the *M. smegmatis* strain grown under P_i-limiting conditions led to merely a slight decrease in *phoA* expression compared with the control strain with pMH201 grown under the same conditions. Western blot analysis revealed that the similar amounts of the WT and K40M mutant forms of PknB-KD^{Mtb} were synthesized in the *M. smegmatis* strains carrying pMHPknB and pMHPknBK40M, respectively. Taken together, these results unequivocally suggest that the inhibitory effect of PknB-KD^{Mtb} overexpression on *phoA* expression was exerted by the increased PknB kinase activity in *M. smegmatis*.

Phosphorylation of Thr-100, Thr-191, and Thr-217 leads to inactivation of RegX3 transcriptional activity

To identify the amino acid residues of RegX3^{Mtb} that are phosphorylated by PknB-KD^{Mtb}, we determined the sites (amino acids) of phosphorylation by LC-electrospray ionization MS/MS using purified RegX3^{Mtb} phosphorylated by purified PknB-KD^{Mtb} (Fig. S4). The phosphorylation reaction was conducted with purified RegX3^{Mtb} and PknB-KD^{Mtb} at a 1:1 stoichiometry for 1 h at 30 °C. The RegX3^{Mtb} protein phosphorylated by PknB-KD^{Mtb} was subjected to MS/MS analysis after in-gel digestion by trypsin, and phosphoresidues were identified from the MS/MS spectra. It was revealed that six Thr residues of RegX3^{Mtb}, corresponding to Thr-29, Thr-100, Thr-151, Thr-191, Thr-193, and Thr-217, were phosphorylated by PknB-KD^{Mtb}. To confirm the MS result, we introduced point mutations (T29E, T100E, T151E, T191E, T193E, and T217E) into RegX3^{Mtb} by site-directed mutagenesis and then performed an *in vitro* phosphorylation assay using the WT and mutant forms of RegX3^{Mtb} and purified PknB-KD^{Mtb}. The phosphorylation reactions were performed with the RegX3^{Mtb} proteins and PknB-KD^{Mtb} at a 2:1 stoichiometry to reduce nonspecific phosphorylation of RegX3^{Mtb}. As shown in Fig. 5, the phosphorylation assay revealed that phosphorylation of T100E and T191E RegX3^{Mtb} by PknB-KD^{Mtb} was significantly reduced compared with of WT RegX3^{Mtb}. Phosphorylation of T217E RegX3^{Mtb} by PknB-KD^{Mtb} was also slightly diminished compared with WT RegX3^{Mtb}. In contrast, the T29E, T151E, and T193E mutations did not affect RegX3^{Mtb} phosphorylation by PknB-KD^{Mtb}. A cumulative effect of T100E and T191E mutations on RegX3^{Mtb} phosphorylation was observed for RegX3^{Mtb} with double mutations (T100E/T191E) (Fig. S5). The T100E/T191E mutant form of RegX3^{Mtb} was only marginally phosphorylated by PknB-KD^{Mtb}, which could be explained by slight phosphorylation of Thr-217. Taken together, these results suggest that Thr-100 and Thr-191 in RegX3^{Mtb} are the major sites of phosphorylation by PknB^{Mtb}. The detection of Thr-29, Thr-151, and Thr-193 phosphorylation in the MS analysis likely resulted from nonspecific phosphorylation of the residues in

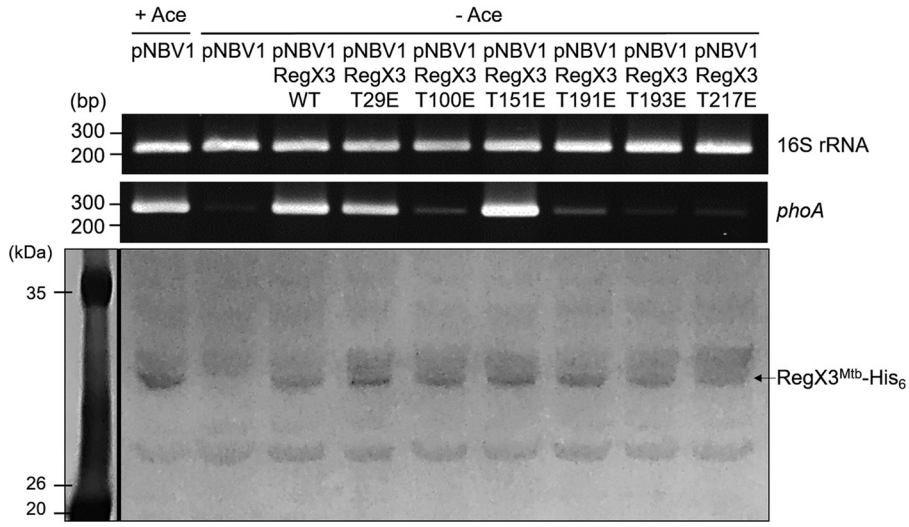

Figure 6. Effect of T29E, T100E, T151E, T191E, T193E, and T217E mutations on the transcriptional activity of RegX3^{Mtb} *in vivo*. The Δ*regX3* conditional mutant strains of *M. smegmatis* with pNBV1RegX3WT, pNBV1RegX3T29E, pNBV1RegX3T100E, pNBV1RegX3T151E, pNBV1RegX3T191E, pNBV1RegX3T193E, or pNBV1RegX3T217E were used for complementation analysis. The complementation test was performed by determining the expression level of *phoA* in *M. smegmatis* strains grown under P_i-limiting conditions in the absence of acetamide by RT-PCR. As a control, the Δ*regX3* conditional mutant with the empty pNBV1 vector, which was grown under P_i-limiting conditions in the absence (−*Ace*) or presence of (+*Ace*) of acetamide, was included in the experiment. RT-PCR for 16S rRNA was conducted to ensure that the same amounts of total RNA were employed for RT-PCR. Protein levels of the WT and mutant forms of RegX3^{Mtb} expressed in the strains were determined by Western blot analysis with a His tag antibody, and the result is shown below the RT-PCR result.

prolonged phosphorylation reactions with excess amounts of PknB-KD^{Mtb}.

To indirectly examine the phosphorylation effects of Thr-29, Thr-100, Thr-151, Thr-191, Thr-193, and Thr-217 on the transcriptional activity of RegX3^{Mtb} *in vivo*, we examined the transcriptional activity of the phosphomimetic mutant (T29E, T100E, T151E, T191E, T193E, and T217E) forms of RegX3^{Mtb} by determining *phoA* expression in the Δ*regX3* conditional mutant of *M. smegmatis* expressing the mutant forms of RegX3^{Mtb} under P_i-limiting conditions (Fig. 6). The Δ*regX3* conditional mutant of *M. smegmatis* was complemented by introducing the pNBV1 derivatives that carry the WT or mutant *regX3*^{Mtb} genes (pNBV1RegX3WT, pNBV1RegX3T29E, pNBV1RegX3T100E, pNBV1RegX3T151E, pNBV1RegX3T191E, pNBV1RegX3T193E, and pNBV1RegX3T217E), and the expression level of *phoA* in the strains grown under P_i-limiting conditions was measured by RT-PCR. As expected, the *phoA* gene was strongly expressed in the Δ*regX3* conditional mutant with the pNBV1 empty vector, which was grown in the presence of acetamide, whereas *phoA* expression occurred only marginally in the same strain grown in the absence of acetamide. In good agreement with this result, Western blot analysis revealed that His_6-tagged RegX3^{Mtb} was detected in the Δ*regX3* conditional mutant grown in the presence of acetamide but not in the mutant strain grown in the absence of acetamide, confirming conditional expression of *regX3*^{Mtb} in the mutant depending on the presence or absence of acetamide. Expression of the WT, T29E, or T151E RegX3^{Mtb} complemented the Δ*regX3* conditional mutant grown in the absence of acetamide, as judged by *phoA* expression, whereas that of T100E, T191E, T193E, and T217E RegX3^{Mtb} did not. Western blot analysis showed that all mutant forms of RegX3^{Mtb} were expressed from the pNBV1 derivatives. The result shown in Fig. 6 implies that phosphorylation of Thr-100, Thr-191, Thr-193, and Thr-217 leads to inactivation of RegX3 transcriptional activity.

To determine whether the DNA-binding affinity of RegX3^{Mtb} is affected by phosphorylation of Thr-100, Thr-191, and Thr-217, we examined the binding of the corresponding phosphomimetic mutant forms (T100E, T191E, and T217E) of RegX3^{Mtb} to DNA fragments containing the upstream regulatory region of *phoA* by EMSA. As shown in Fig. 7*A*, more DNA fragments were shifted with increasing concentrations of WT and T100E RegX3^{Mtb}. In contrast, almost no band shift was observed for T191E RegX3^{Mtb}, and only a marginal band shift occurred for T217E RegX3^{Mtb} at high concentrations of the protein. To directly ascertain whether phosphorylation of RegX3^{Mtb} influences its DNA binding affinity, we performed EMSA using the RegX3^{Mtb} protein subjected to the phosphorylation reactions with the WT or K40M mutant form of PknB-KD^{Mtb}. When the phosphorylation reaction of RegX3^{Mtb} was done without PknB-KD^{Mtb}, the DNA fragments with the *phoA* upstream region were shifted in the EMSA (Fig. 7*B*). Phosphorylation of RegX3^{Mtb} by the active PknB-KD^{Mtb} abolished binding of RegX3^{Mtb} to the DNA fragments, whereas RegX3^{Mtb} subjected to the phosphorylation reaction with the inactive K40M PknB-KD^{Mtb} retained its DNA-binding ability. The WT or mutant form of PknB-KD^{Mtb} alone without RegX3^{Mtb} did not bind to the DNA fragments. Taken together, the results in Fig. 7 suggest that phosphorylation of RegX3^{Mtb} on Thr-191 and Thr-217 by PknB^{Mtb} significantly reduces the binding affinity of RegX3^{Mtb} for its target DNA sequence whereas phosphorylation of RegX3^{Mtb} on Thr-100 by PknB^{Mtb} does not.

Discussion

The *pknB* gene forms an operon with *pknA*, *pbpA*, *rodA*, *pstP* (encoding a metal-dependent Ser/Thr protein phosphatase), and two genes coding for forkhead-associated domain–containing proteins. This genetic locus was found to be conserved near the replication origin in the chromosomes of Acti-

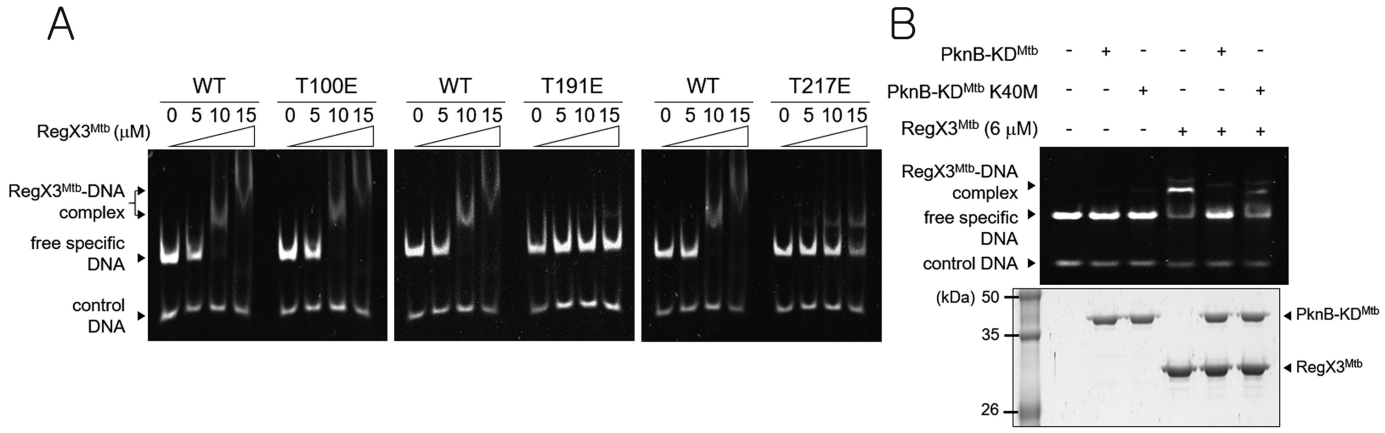

Figure 7. Binding of the purified WT, T100E, T191E, and T217E mutant forms of RegX3^{Mtb} to the *phoA* upstream region and the effect of RegX3^{Mtb} phosphorylation by PknB-KD^{Mtb} on the DNA binding affinity of RegX3^{Mtb}. *A*, 100 fmol each of 123-bp DNA fragments containing a RegX3-binding site upstream of *phoA* (*specific DNA*) and 60-bp DNA fragments without a RegX3-binding site (*control DNA*) were used in an EMSA with various concentrations of purified WT, T100E, T191E, or T217E RegX3^{Mtb}. RegX3^{Mtb}–DNA reaction mixtures were incubated for 20 min at 25 °C. The RegX3^{Mtb}–DNA reaction mixtures were subjected to native PAGE (6% (w/v) acrylamide gel). The gels for the EMSA were stained with SYBR Green staining solution after electrophoresis. The concentrations of WT, T100E, T191E, and T217E RegX3^{Mtb} used in the EMSA are shown above the lanes. *B*, to phosphorylate RegX3^{Mtb}, 120 pmol of RegX3^{Mtb} was incubated with 60 pmol of WT PknB-KD^{Mtb} in 16 μl of reaction buffer (20 mM Tris-Cl (pH 7.5), 50 mM NaCl, 10 mM $MgCl_2$, and 10 mM $MnCl_2$) containing 100 μM ATP for 1 h at 30 °C. As a negative control, inactive K40M PknB-KD^{Mtb} was employed instead of WT PknB-KD^{Mtb}. 4 μl of the DNA mixture containing 200 fmol each of specific and control DNA fragments was added to 16 μl of the above phosphorylation reaction mixtures and incubated for 20 min at 25 °C. 10 μl of the DNA-binding reaction mixtures were used for the EMSA, and 10 μl of the remaining reaction mixtures were subjected to SDS-PAGE to see the amounts of RegX3^{Mtb} and PknB-KD^{Mtb} used in the EMSA. The CBB-stained gel used for SDS-PAGE is presented below the EMSA result.

nobacteria, including mycobacteria (34, 55, 56). PknA and PknB have been suggested to be essential STPKs for mycobacteria and to be implicated in signal transduction regulating cell wall synthesis and cell shape (38, 39, 57–60). PknB is composed of the N-terminal KD and the C-terminal extracytoplasmic domain consisting of four penicillin-binding protein and Ser/Thr kinase–associated (PASTA) repeats (61). These kinds of PASTA repeats are also found in PknB-like STPKs of Gram-positive bacteria, including Actinobacteria (62, 63). Several lines of evidence for phosphorylation of RRs by STPKs in mycobacteria have been reported. In 2010, phosphorylation of the DosR (DevR) RR by PknH was first reported in *Mtb* (43). PknH has been demonstrated to phosphorylate DosR (DevR) on Thr-198 and Thr-205 to enhance DosR (DevR) transcriptional activity. Recently, we revealed that purified PknB-KD^{Mtb} strongly phosphorylated six RRs (RegX3, NarL, KdpE, TrcR, DosR/DevR, and MtrA) of *Mtb in vitro*. Based on this finding, we began to study signal convergence between PknB and TCSs in mycobacteria and demonstrated that overexpression of PknB-KD^{Mtb} in *M. smegmatis* resulted in a significant inhibition of DosR (DevR) transcriptional activity by phosphorylating Thr-180 of DosR (DevR) (50). We chose the SenX3–RegX3 TCS to further study the cross-talk between PknB and TCSs in mycobacteria because well-known reporter genes such as *phoA* and *pstS*, which are under strict control of the SenX3–RegX3 TCS, were available to determine the transcriptional activity of RegX3, and the activation condition of the SenX3–RegX3 TCS (P_i-limiting condition) was established (14).

We observed that the transcriptional activity of RegX3^{Ms} and RegX3^{Mtb} was reduced with increased expression and activity of PknB-KD^{Mtb} (Figs. 2–4). Furthermore, MS/MS analysis following the *in vitro* phosphorylation reaction with purified RegX3^{Mtb} and PknB-KD^{Mtb} led to detection of six phosphorylation sites (Thr-29, Thr-100, Thr-151, Thr-191, Thr-193, and Thr-217) on RegX3^{Mtb} (Fig. S4). Because our MS/MS results did not show the phosphorylation extent of the identified Thr residues, we performed an *in vitro* phosphorylation assay with nonphosphorylatable Thr-to-Glu mutant forms of RegX3^{Mtb} and purified PknB-KD^{Mtb} (Fig. 5), which revealed that Thr-100 and Thr-191 of RegX3^{Mtb} are the major sites of phosphorylation, whereas Thr-217 is the minor phosphorylation site. In addition, the phosphomimetic T100E, T191E, and Thr217E mutant forms of RegX3^{Mtb} were shown to lose transcriptional activity, as judged by the complementation result (Fig. 6). Altogether, these results indicate that PknB kinase activity inhibits the transcriptional activity of RegX3^{Mtb} mainly through phosphorylation of Thr-100 and Thr-191 (Thr-98 and Thr-189 in the case of RegX3^{Ms}), which are located in the receiver domain and the DNA-binding helix–turn–helix motif of RegX3, respectively (Fig. S6). From the location of Thr-191 on RegX3^{Mtb}, it was assumed that phosphorylation of Thr-191 might inhibit the transcriptional activity of RegX3^{Mtb} by perturbing DNA binding of RegX3^{Mtb}. Indeed, our EMSA revealed that the phosphomimetic T191E mutation in RegX3^{Mtb} led to abolishment of the DNA-binding ability of RegX3^{Mtb} (Fig. 7). The location of Thr-217 near the helix–turn–helix motif accounts for abolishment of the transcriptional activity and DNA-binding ability of T217E RegX3^{Mtb}. Despite the lack of its transcriptional activity, the T100E mutant form of RegX3^{Mtb} has been shown to retain the same degree of DNA-binding ability as the WT form of RegX3^{Mtb} (Fig. 7), indicating that the lack of transcriptional activity of T100E RegX3^{Mtb} is not the result of its inability to bind DNA. The RR of the TCS contains six well-conserved residues (three acidic amino acids, one Thr/Ser, one Tyr/Phe, and one Lys) that are functionally important for phosphorylation of the RR and activation of the effector domain through phosphorylation-induced conformational changes (64–66). In the case of RegX3^{Mtb}, the six residues correspond to Glu-8, Asp-9, Asp-52, Thr-79, Tyr-98, and Lys-101. The location of Thr-100 between Tyr-98 and Lys-101 implies that the

T100E mutation (and, therefore, phosphorylation of Thr-100 by PknB) is likely to make it unlikely that RegX3^{Mtb} is activated through phosphorylation-induced conformational changes.

As mentioned above, six RRs of the 11 paired TCSs found in *Mtb* were shown to be robustly phosphorylated by PknB-KD^{Mtb}. Four (RegX3, KdpE, TrcR, and MtrA) of the six RRs are structurally related to the OmpR family of RRs. The Thr residues corresponding to Thr-191 and Thr-217 of RegX3^{Mtb} are conserved in the four RRs (RegX3, KdpE, TrcR, and MtrA), whereas the Thr-100 – corresponding residues are conserved in RegX3, KdpE, and TrcR but not in MtrA (Fig. S6). Given the strong phosphorylation of KdpE, TrcR, and MtrA by PknB-KD^{Mtb} like RegX3 and the conservation of at least two of three Thr residues corresponding to Thr-100, Thr-191, and Thr-217 of RegX3^{Mtb}, as well as the good conservation of amino acid sequences around the Thr residues corresponding to Thr-100 of RegX3^{Mtb}, it is possible that PknB might inhibit the transcriptional activity of KdpE, TrcR, and MtrA as well.

The signal convergence between TCSs and STPKs was also observed in several Gram-positive bacteria besides mycobacteria. In most cases, an STPK phosphorylates an RR to change the transcriptional activity of the RR. The WalR RR of the WalKR TCS in *Bacillus subtilis* has been reported to be phosphorylated by PrkC (a PknB homolog) both *in vitro* and *in vivo* (49). WalR shares a relatively high sequence similarity (48% identity and 81% similarity) with RegX3^{Mtb} over the whole protein sequence (Fig. S7). Phosphorylation of WalR on Thr-101, which corresponds to Thr-100 of RegX3^{Mtb}, has been shown to cause changes in WalR transcriptional activity. It is noteworthy that the amino acid residues around the Thr residues are very well conserved in WalR and RegX3 (Fig. S7), which reinforces phosphorylation of RegX3^{Mtb} on Thr-100 by PknB. In group A and group B streptococci, phosphorylation of the CovR RR on Thr-65 by a PknB-like STPK (Stk or Stk1) has been shown to inhibit acetyl phosphate– dependent phosphorylation of CovR (41, 48). The RR06 and RitR RRs of *Streptococcus pneumoniae* have been shown to be phosphorylated by a PknB-like STPK, StkP (42, 45). The GraR RR of the GraSR TCS of *Staphylococcus aureus* has been demonstrated to be phosphorylated on Thr-128, Thr-130, and Thr-149 by Stk1, which resulted in an increase in the DNA-binding affinity of GraR (46). Phosphorylation of the VraR RR of the *S. aureus* VraSR TCS on Thr-106 and Thr-119 in the receiver domain and on Thr-175 and Thr-178 within the DNA-binding domain by Stk1 has been shown to reduce its DNA binding affinity (47). The observation that several RRs are phosphorylated by multiple kinases, including their cognate HKs and STPKs, suggests that signaling through TCSs in bacteria could be more complex than anticipated.

The PASTA repeats of PknB have been demonstrated to serve as binding modules for muropeptides of peptidoglycan, and binding of muropeptides to the PASTA repeats has been suggested to activate PknB kinase activity (67). PknB has been demonstrated to be localized to the septa and poles of the dividing bacterial cell, where higher local concentrations of muropeptides are available because of high rates of peptidoglycan turnover and synthesis (54, 68). These facts, in conjunction with the observation that the cellular abundance of PknB is significantly reduced in the nonreplicating *Mtb* cells relative to that in actively dividing cells (69), suggest that the kinase activity of PknB might be much higher in actively dividing mycobacteria than in nonreplicating mycobacteria, which raises the possibility that PknB might play a role in the regulation of gene expression and cellular processes as a sensor kinase that coordinates the replication state with the regulation of intracellular metabolism and gene expression in mycobacteria.

From this viewpoint, we propose a model for the dual control of RegX3 transcriptional activity by SenX3 and PknB. The major sensory kinase regulating the transcriptional activity of RegX3 in response to P_i availability is the SenX3 HK. Under favorable growth conditions with sufficient P_i supplementation, the RegX3 RR is not activated by the SenX3 HK, and the high activity of PknB might further inhibit the residual transcriptional activity of RegX3 by functioning as an "auxiliary switch" or "safety lock" to minimize leaky expression of the RegX3 regulon. Under P_i-limiting conditions, where RegX3 is activated by SenX3, reduced PknB activity because of inhibited replication of mycobacterial cells might mitigate the inhibitory effect of PknB on RegX3, enabling full activation of RegX3 transcriptional activity.

In conclusion, we found that overexpression of PknB-KD^{Mtb} inhibits the transcriptional activity of RegX3^{Mtb} by phosphorylating Thr-100, Thr-191, and Thr-217 (Thr-98, Thr-189, and Thr-215 for RegX3^{Ms}). Convergence of the PknB and SenX3-RegX3 signaling pathways might enable mycobacteria to integrate two different signals, the environmental P_i level and the replication state, to regulate gene expression in response to changing P_i availability.

Experimental procedures

Bacterial strains, plasmids, and culture conditions

The bacterial strains and plasmids used in this study are listed in Table S1. *Escherichia coli* strains were grown in Luria–Bertani medium at 37 °C. *M. smegmatis* strains were grown in Middlebrook 7H9 medium (Difco, Detroit, MI) supplemented with 0.2% (w/v) glucose as a carbon source and 0.02% (v/v) Tween 80 as an anticlumping agent at 37 °C. For P_i-limiting and replete growth conditions, MOPS minimal medium (25 mM MOPS (pH 7.2), 25 mM KCl, 10 mM Na_2SO_4, 20 mM NH_4Cl, 10 μM $FeCl_3$, 2 mM $MgSO_4$, and 0.1 mM $CaCl_2$) supplemented with 50 μM and 10 mM K_2HPO_4, respectively, were used. *M. smegmatis* strains were grown aerobically on a gyratory shaker (200 rpm) to an A_{600} of 0.4–0.5. Ampicillin (100 μg/ml for *E. coli*), kanamycin (50 μg/ml for *E. coli* and 15 or 30 μg/ml for *M. smegmatis*), and hygromycin (200 μg/ml for *E. coli* and 50 μg/ml for *M. smegmatis*) were added to the growth medium when required. Overexpression of the genes encoding PknB-KD^{Mtb} and RegX3^{Mtb} from pMH201-derived plasmids was induced by addition of acetamide to the growth medium to a final concentration of 0.2% (w/v) unless specific concentrations of acetamide are stated. Construction of the plasmids and a Δ*regX3* conditional mutant of *M. smegmatis* is described in the supporting information.

Determination of colony-forming units

Samples (1 ml) were collected from *M. smegmatis* cultures at the indicated time points. The collected samples were homoge-

neously resuspended by passing them ten times through a 25-gauge needle to break up cell clumps. 200 μl of the samples appropriately diluted with MOPS minimal medium were plated on glucose–MOPS agar plates supplemented with either 10 mM or 50 μM K_2HPO_4 and 0.2% (w/v) acetamide. The bacterial colonies growing on agar plates were counted after 72-h incubation at 37 °C.

DNA manipulation and electroporation

Recombinant DNA manipulations were conducted in accordance with standard protocols and the manufacturer's instructions (70). Transformation of *M. smegmatis* with plasmids was carried out by electroporation as described previously (71).

Site-directed mutagenesis

To introduce point mutations into the genes encoding $RegX3^{Mtb}$ and $PknB\text{-}KD^{Mtb}$, PCR-based mutagenesis was conducted using the QuikChange site-directed mutagenesis procedure (Stratagene, La Jolla, CA). Synthetic oligonucleotides 33 bases long and containing a mutated codon in the middle of their sequences were used to mutagenize the original codons (Table S2). Mutations were verified by DNA sequencing.

β-Galactosidase activity assay and determination of protein concentration

β-Galactosidase activity was measured spectrophotometrically as described elsewhere (72). A Bio-Rad protein assay kit was used to determine the protein concentration.

RT-PCR and real-time qPCR

RNA isolation from *M. smegmatis* strains, preparation of complementary DNA, RT-PCR, and real-time qPCR were conducted as described previously (73). The primers used for complementary DNA synthesis, RT-PCR, and real-time qPCR are listed in Table S2.

Protein purification

E. coli strains overexpressing $RegX3^{Mtb}$ or $PknB\text{-}KD^{Mtb}$ were grown aerobically at 37 °C in Luria–Bertani medium containing 100 μg/ml ampicillin (for *E. coli* strains containing the pT7–7 derivatives) or 50 μg/ml kanamycin (for the *E. coli* strain carrying pETpknBhis) to an A_{600} of 0.4–0.6. Expression of the $regX3^{Mtb}$ and $pknB^{Mtb}$ genes was induced by addition of IPTG to a final concentration of 0.5 mM, and then cells were grown further for 4 h at 30 °C. Harvested cells from 200 ml of culture were resuspended in 5 ml of buffer A (20 mM Tris-Cl (pH 8.0) and 100 mM NaCl) in the presence of DNase I (10 units/ml) and 10 mM $MgCl_2$ and disrupted by two passages through a French pressure cell. Cell-free crude extracts were obtained by centrifugation twice at 23,708 × *g* for 15 min. 500 μl of the 50% (v/v) slurry (bed volume, 250 μl) of Ni-Sepharose high-performance resin (GE Healthcare) was packed into a column. After equilibration of the resin with 10 bed volumes of buffer A, cell-free crude extracts were loaded into the column. The resin was washed with 60 bed volumes of buffer A containing 5 mM imidazole and 60 bed volumes of buffer A containing 10 mM imidazole, and then His_6-tagged $RegX3^{Mtb}$ and His_6-tagged $PknB\text{-}KD^{Mtb}$ were finally eluted with 10 bed volumes of buffer A containing 250 mM imidazole. The eluted proteins were desalted using a PD-10 desalting column (GE Healthcare) equilibrated with the appropriate buffer.

Western blot analysis

To determine the amount of expressed His_6-tagged $RegX3^{Mtb}$ and $PknB\text{-}KD^{Mtb}$ in cells, Western blot analysis was performed as described previously (74). To detect His_6-tagged proteins, mouse monoclonal IgG against His-3 (Santa Cruz Biotechnology, Santa Cruz, CA; sc8036) was used at a 1:2,000 dilution. Alkaline phosphatase–conjugated anti-mouse IgG produced in rabbits (Sigma, A4312) was used at a 1:10,000 dilution for detection of the primary antibody.

Analysis of in vivo protein–protein interactions

Saccharomyces cerevisiae AH109 strains cotransformed with both the pGADT7linker and pGBKT7 derivatives were grown in synthetic defined dropout (SD) medium (Clontech, Palo Alto, CA) lacking leucine and tryptophan (SD/−Leu/−Trp). The overnight cultures were diluted with distilled water to an A_{600} of 0.6 and spotted onto both solid SD/−Leu/−Trp plates and histidine-deficient SD/−Leu/−Trp/−His plates for a spotting assay. These plates were incubated at 30 °C for 3–5 days.

In vitro kinase assay

Purified $PknB\text{-}KD^{Mtb}$ was mixed with purified WT or mutant forms of $RegX3^{Mtb}$ in 20 μl of reaction buffer (20 mM Tris-Cl (pH 7.5), 50 mM NaCl, 10 mM $MgCl_2$, and 10 mM $MnCl_2$). Reactions were started by adding 100 μM cold ATP and 1,000 Ci/mol [γ-^{32}P]ATP and incubated at 30 °C. The reactions were terminated at the indicated time points by adding 5 μl of gel-loading buffer (250 mM Tris-Cl (pH 6.8), 50% (w/v) glycerol, 500 mM DTT, 10% (w/v) SDS, 5% (v/v) β-mercaptoethanol, and 0.5% (w/v) bromphenol blue) containing 100 mM EDTA. Proteins were resolved by SDS-PAGE. The gels were dried and exposed to films at room temperature overnight.

LC-MS/MS analysis for phosphorylated $RegX3^{Mtb}$

Phosphorylation reactions of 0.4 nmol of WT $RegX3^{Mtb}$ were conducted in the presence of 0.4 nmol of $PknB\text{-}KD^{Mtb}$ in 84 μl of reaction buffer (20 mM Tris-Cl (pH 7.5), 50 mM NaCl, 10 mM $MgCl_2$, 10 mM $MnCl_2$, and 100 μM ATP) for 1 h at 30 °C. The reactions were terminated by adding 30 μl of gel-loading buffer containing 100 mM EDTA. The proteins were subjected to SDS-PAGE and stained with Coomassie Brilliant Blue (CBB), and the $RegX3^{Mtb}$ bands were excised. The excised protein bands from SDS-PAGE gels were cut into small pieces, washed three times with 200 μl of HPLC-grade water, and destained with 200 μl of 1:1 (v:v) mixture of acetonitrile and ammonium bicarbonate (100 mM (pH 8.0)). The gel pieces were dehydrated for 5 min with 500 μl of 100% acetonitrile and incubated in a solution of 10 mM DTT in 100 mM ammonium bicarbonate (50 μl) for 30 min at 56 °C, followed by 55 mM iodoacetamide in 100 mM ammonium bicarbonate (50 μl) for 20 min at room temperature in the dark. Thereafter, the gel pieces were dehydrated again with 100% acetonitrile and rehydrated in a solution of 13 ng/μl of sequencing-grade modified trypsin (Promega, Madi-

son, WI) in 10 mM ammonium bicarbonate. The digestion was completed overnight at 37 °C. Peptides were extracted by incubating the gel pieces in a 1:2 (v:v) mixture of 5% formic acid and acetonitrile, and the solution was dried by vacuum centrifugation.

Peptide samples were reconstituted in 7 μl of 0.1% formic acid and injected from an auto sampler into a reverse-phase C_{18} column (20 cm × 75 μm inner diameter, 3 μm, 300 Å, packed in-house; Dr. Maisch GmbH) on an Eksigent multidimensional liquid chromatography system at a flow rate of 300 nl/min. Before use, the column was equilibrated with 95% mobile phase A (0.1% formic acid in H_2O) and 5% mobile phase B (0.1% formic acid in acetonitrile). The peptides were eluted with a linear gradient from 10%–35% B over 100 min, followed by washing with 70% B and re-equilibration with 5% B at a flow rate of 300 nl/min with a total run time of 130 min. The HPLC system was connected to an LTQ Orbitrap XL mass spectrometer (Thermo Fisher Scientific, Waltham, MA) operated in data-dependent acquisition mode. Survey full-scan MS spectra (m/z 400–2,000) were acquired in the Orbitrap with a resolution of 60,000. Source ionization parameters were as follows: spray voltage, 1.9 kV; capillary temperature, 275 °C. The MS/MS spectra of the 10 most intense ions from the MS1 scan with a charge state of 1 or more were acquired in the ion trap with the following options: isolation width, 2.0 m/z; normalized collision energy, 45%; dynamic exclusion, 60 s.

The acquired MS/MS spectra were subjected to a search against the in-house database (containing $RegX3^{Mtb}$ and PknB-KD^{Mtb} sequences with a common contaminant database) using the SEQUEST HT software in Proteome Discoverer 2.2 (Thermo Fisher Scientific). Two missed trypsin cleavages were allowed, and the peptide mass tolerances for MS/MS and MS were set to ±0.6 Da and ±10 ppm, respectively. Other parameters used for the SEQUEST HT searches included fixed modification of carbamidomethylation at cysteine (+57.02 Da), variable modification of oxidation at methionines (+15.99 Da), and phosphorylation at serine, threonine, or tyrosine (+79.97 Da). *ptm*RS was run in PhosphoRS mode to localize the phosphorylation site. A probability of 75% or higher was considered to confidently indicate a phosphorylation site.

EMSA

123-bp DNA fragments including a RegX3-binding site upstream of the *phoA* gene were used in the assay (specific DNA). The DNA fragments were generated by PCR using the primer set F_phoA_EMSA_123 (5′-AGTCAAGCTTGCTCTCGACGCCGTCGTG-3′) and R_phoA_EMSA_123 (5′-AGTCGAATTCTGATCGCGAGTCACATAAGC-3′) and pNC-phoA as a template. 60-bp control DNA fragments without the RegX3-binding site were amplified by PCR using pUC19 as a template (control DNA) and the primers pUC19_EMSA_F (5′-CCTCTAGAGTCGACCTGC-3′) and pUC19_EMSA_R (5′-AGGAAACAGCTATGACCATG-3′). Purified $RegX3^{Mtb}$ proteins were incubated with 100 fmol each of specific and control DNA in buffer (20 mM MOPS (pH 8.0) containing 150 mM KCl) in a final volume of 10 μl for 20 min at 25 °C. To examine the effect of $RegX3^{Mtb}$ phosphorylation by PknB-KD^{Mtb} on DNA binding, phosphorylation reactions were performed in 10 μl of kinase buffer (20 mM Tris-Cl (pH 7.5), 25 mM NaCl, 10 mM $MgCl_2$, and 20 mM $MnCl_2$) and 100 μM ATP containing 60 pmol of $RegX3^{Mtb}$ and 30 pmol of the WT or mutant form (K40M) of PknB-KD^{Mtb} for 30 min at 30 °C, and then 100 fmol each of the specific and control DNA were added to the phosphorylation reaction mixtures. The binding reaction mixtures were incubated for 20 min at 25 °C. After addition of 2 μl of 6× loading buffer (0.25% (w/v) bromphenol blue, 0.25% (w/v) xylene cyanol, and 40% (w/v) sucrose), the mixtures were subjected to nondenaturing PAGE (6% (w/v) acrylamide) using 0.5× TBE buffer (41.5 mM Tris borate and 0.5 mM EDTA (pH 8.3)) at 50 V/cm for 1 h 50 min at 4 °C. The gels were stained with SYBR Green staining solution (Invitrogen) for 30 min. Bands were visualized using an UV illuminator.

Author contributions—E.-J. P. and Y.-M. K. data curation; E.-J. P. and J.-I. O. validation; E.-J. P. and Y.-M. K. investigation; E.-J. P. and Y.-M. K. writing-original draft; J.-W. L., H.-Y. K., and J.-I. O. supervision; J.-W. L., H.-Y. K., and J.-I. O. writing-review and editing; J.-I. O. conceptualization; J.-I. O. resources; J.-I. O. formal analysis; J.-I. O. funding acquisition.

References

1. Chakraborti, P. K., Matange, N., Nandicoori, V. K., Singh, Y., Tyagi, J. S., and Visweswariah, S. S. (2011) Signalling mechanisms in mycobacteria. *Tuberculosis* **91,** 432–440 CrossRef Medline
2. Schnappinger, D., Ehrt, S., Voskuil, M. I., Liu, Y., Mangan, J. A., Monahan, I. M., Dolganov, G., Efron, B., Butcher, P. D., Nathan, C., and Schoolnik, G. K. (2003) Transcriptional adaptation of *Mycobacterium tuberculosis* within macrophages: insights into the phagosomal environment. *J. Exp. Med.* **198,** 693–704 CrossRef Medline
3. Graves, J. D., and Krebs, E. G. (1999) Protein phosphorylation and signal transduction. *Pharmacol. Ther.* **82,** 111–121 CrossRef Medline
4. Sridhar, R., Hanson-Painton, O., and Cooper, D. R. (2000) Protein kinases as therapeutic targets. *Pharm. Res.* **17,** 1345–1353 CrossRef Medline
5. Stock, A. M., Robinson, V. L., and Goudreau, P. N. (2000) Two-component signal transduction. *Annu. Rev. Biochem.* **69,** 183–215 CrossRef Medline
6. West, A. H., and Stock, A. M. (2001) Histidine kinases and response regulator proteins in two-component signaling systems. *Trends Biochem. Sci.* **26,** 369–376 CrossRef Medline
7. Jung, K., Fried, L., Behr, S., and Heermann, R. (2012) Histidine kinases and response regulators in networks. *Curr. Opin. Microbiol.* **15,** 118–124 CrossRef Medline
8. Zschiedrich, C. P., Keidel, V., and Szurmant, H. (2016) Molecular mechanisms of two-component signal transduction. *J. Mol. Biol.* **428,** 3752–3775 CrossRef Medline
9. Mascher, T., Helmann, J. D., and Unden, G. (2006) Stimulus perception in bacterial signal-transducing histidine kinases. *Microbiol. Mol. Biol. Rev.* **70,** 910–938 CrossRef Medline
10. Gao, R., Mack, T. R., and Stock, A. M. (2007) Bacterial response regulators: versatile regulatory strategies from common domains. *Trends Biochem. Sci.* **32,** 225–234 CrossRef Medline
11. Cole, S. T., Brosch, R., Parkhill, J., Garnier, T., Churcher, C., Harris, D., Gordon, S. V., Eiglmeier, K., Gas, S., Barry, C. E., 3rd, Tekaia, F., Badcock, K., Basham, D., Brown, D., Chillingworth, T., *et al.* (1998) Deciphering the biology of *Mycobacterium tuberculosis* from the complete genome sequence. *Nature* **393,** 537–544 CrossRef Medline
12. Parish, T. (2014) Two-component regulatory systems of mycobacteria. *Microbiol. Spectr.* **2,** MGM2-0010-2013 Medline
13. Kundu, M. (2018) The role of two-component systems in the physiology of *Mycobacterium tuberculosis*. *IUBMB Life* **70,** 710–717 CrossRef Medline
14. Glover, R. T., Kriakov, J., Garforth, S. J., Baughn, A. D., and Jacobs, W. R., Jr. (2007) The two-component regulatory system *senX3-regX3* regulates

phosphate-dependent gene expression in *Mycobacterium smegmatis*. *J. Bacteriol.* **189,** 5495–5503 Medline
15. Rifat, D., Bishai, W. R., and Karakousis, P. C. (2009) Phosphate depletion: a novel trigger for *Mycobacterium tuberculosis* persistence. *J. Infect. Dis.* **200,** 1126–1135 CrossRef Medline
16. Parish, T., Smith, D. A., Kendall, S., Casali, N., Bancroft, G. J., and Stoker, N. G. (2003) Deletion of two-component regulatory systems increases the virulence of *Mycobacterium tuberculosis*. *Infect. Immun.* **71,** 1134–1340 CrossRef Medline
17. Parish, T., Smith, D. A., Roberts, G., Betts, J., and Stoker, N. G. (2003) The *senX3-regX3* two-component regulatory system of *Mycobacterium tuberculosis* is required for virulence. *Microbiology* **149,** 1423–1435 CrossRef Medline
18. Rickman, L., Saldanha, J. W., Hunt, D. M., Hoar, D. N., Colston, M. J., Millar, J. B., and Buxton, R. S. (2004) A two-component signal transduction system with a PAS domain-containing sensor is required for virulence of *Mycobacterium tuberculosis* in mice. *Biochem. Biophys. Res. Commun.* **314,** 259–267 CrossRef Medline
19. Tischler, A. D., Leistikow, R. L., Kirksey, M. A., Voskuil, M. I., and McKinney, J. D. (2013) *Mycobacterium tuberculosis* requires phosphate-responsive gene regulation to resist host immunity. *Infect. Immun.* **81,** 317–328 CrossRef Medline
20. Namugenyi, S. B., Aagesen, A. M., Elliott, S. R., and Tischler, A. D. (2017) *Mycobacterium tuberculosis* PhoY proteins promote persister formation by mediating Pst/SenX3-RegX3 phosphate sensing. *MBio* **8,** e00494-17 Medline
21. Singh, N., and Kumar, A. (2015) Virulence factor SenX3 is the oxygen-controlled replication switch of *Mycobacterium tuberculosis*. *Antioxid. Redox Signal.* **22,** 603–613 CrossRef Medline
22. White, D. W., Elliott, S. R., Odean, E., Bemis, L. T., and Tischler, A. D. (2018) *Mycobacterium tuberculosis* Pst/SenX3-RegX3 regulates membrane vesicle production independently of ESX-5 activity. *MBio* **9,** e00778-00718 Medline
23. Lefèvre, P., Braibant, M., de Wit, L., Kalai, M., Röeper, D., Grötzinger, J., Delville, J. P., Peirs, P., Ooms, J., Huygen, K., and Content, J. (1997) Three different putative phosphate transport receptors are encoded by the *Mycobacterium tuberculosis* genome and are present at the surface of *Mycobacterium bovis* BCG. *J. Bacteriol.* **179,** 2900–2906 CrossRef Medline
24. Kriakov, J., Lee, S., and Jacobs, W. R., Jr. (2003) Identification of a regulated alkaline phosphatase, a cell surface-associated lipoprotein, in *Mycobacterium smegmatis*. *J. Bacteriol.* **185,** 4983–4991 CrossRef Medline
25. Brokaw, A. M., Eide, B. J., Muradian, M., Boster, J. M., and Tischler, A. D. (2017) *Mycobacterium smegmatis* PhoU proteins have overlapping functions in phosphate signaling and are essential. *Front. Microbiol.* **8,** 2523–2536 CrossRef Medline
26. Gardner, S. G., Johns, K. D., Tanner, R., and McCleary, W. R. (2014) The PhoU protein from *Escherichia coli* interacts with PhoR, PstB, and metals to form a phosphate-signaling complex at the membrane. *J. Bacteriol.* **196,** 1741–1752 CrossRef Medline
27. Baek, J. H., Kang, Y. J., and Lee, S. Y. (2007) Transcript and protein level analyses of the interactions among PhoB, PhoR, PhoU and CreC in response to phosphate starvation in *Escherichia coli*. *FEMS Microbiol. Lett.* **277,** 254–259 CrossRef Medline
28. Chakraborty, S., Sivaraman, J., Leung, K. Y., and Mok, Y. K. (2011) Two-component PhoB-PhoR regulatory system and ferric uptake regulator sense phosphate and iron to control virulence genes in type III and VI secretion systems of *Edwardsiella tarda*. *J. Biol. Chem.* **286,** 39417–39430 CrossRef Medline
29. Muñoz-Dorado, J., Inouye, S., and Inouye, M. (1991) A gene encoding a protein serine threonine kinase is required for normal development of *M. xanthus*, a Gram-negative bacterium. *Cell* **67,** 995–1006 CrossRef Medline
30. Pereira, S. F., Goss, L., and Dworkin, J. (2011) Eukaryote-like serine/threonine kinases and phosphatases in bacteria. *Microbiol. Mol. Biol. Rev.* **75,** 192–212 CrossRef Medline
31. Cousin, C., Derouiche, A., Shi, L., Pagot, Y., Poncet, S., and Mijakovic, I. (2013) Protein-serine/threonine/tyrosine kinases in bacterial signaling and regulation. *FEMS Microbiol. Lett.* **346,** 11–19 CrossRef Medline
32. Wright, D. P., and Ulijasz, A. T. (2014) Regulation of transcription by eukaryotic-like serine-threonine kinases and phosphatases in Gram-positive bacterial pathogens. *Virulence* **5,** 863–885 CrossRef Medline
33. Khan, M. Z., Kaur, P., and Nandicoori, V. K. (2018) Targeting the messengers: serine/threonine protein kinases as potential targets for antimycobacterial drug development. *IUBMB Life* **70,** 889–904 CrossRef Medline
34. Narayan, A., Sachdeva, P., Sharma, K., Saini, A. K., Tyagi, A. K., and Singh, Y. (2007) Serine threonine protein kinases of mycobacterial genus: phylogeny to function. *Physiol. Genomics* **29,** 66–75 CrossRef Medline
35. Fernandez, P., Saint-Joanis, B., Barilone, N., Jackson, M., Gicquel, B., Cole, S. T., and Alzari, P. M. (2006) The Ser/Thr protein kinase PknB is essential for sustaining mycobacterial growth. *J. Bacteriol.* **188,** 7778–7784 CrossRef Medline
36. Forti, F., Crosta, A., and Ghisotti, D. (2009) Pristinamycin-inducible gene regulation in mycobacteria. *J. Biotechnol.* **140,** 270–277 CrossRef Medline
37. Chawla, Y., Upadhyay, S., Khan, S., Nagarajan, S. N., Forti, F., and Nandicoori, V. K. (2014) Protein kinase B (PknB) of *Mycobacterium tuberculosis* is essential for growth of the pathogen *in vitro* as well as for survival within the host. *J. Biol. Chem.* **289,** 13858–13875 CrossRef Medline
38. Kang, C. M., Abbott, D. W., Park, S. T., Dascher, C. C., Cantley, L. C., and Husson, R. N. (2005) The *Mycobacterium tuberculosis* serine/threonine kinases PknA and PknB: substrate identification and regulation of cell shape. *Genes Dev.* **19,** 1692–1704 CrossRef Medline
39. Gee, C. L., Papavinasasundaram, K. G., Blair, S. R., Baer, C. E., Falick, A. M., King, D. S., Griffin, J. E., Venghatakrishnan, H., Zukauskas, A., Wei, J. R., Dhiman, R. K., Crick, D. C., Rubin, E. J., Sassetti, C. M., and Alber, T. (2012) A phosphorylated pseudokinase complex controls cell wall synthesis in mycobacteria. *Sci. Signal.* **5,** ra7 Medline
40. Ortega, C., Liao, R., Anderson, L. N., Rustad, T., Ollodart, A. R., Wright, A. T., Sherman, D. R., and Grundner, C. (2014) *Mycobacterium tuberculosis* Ser/Thr protein kinase B mediates an oxygen-dependent replication switch. *PLoS Biol.* **12,** e1001746 CrossRef Medline
41. Lin, W. J., Walthers, D., Connelly, J. E., Burnside, K., Jewell, K. A., Kenney, L. J., and Rajagopal, L. (2009) Threonine phosphorylation prevents promoter DNA binding of the Group B *Streptococcus* response regulator CovR. *Mol. Microbiol.* **71,** 1477–1495 CrossRef Medline
42. Ulijasz, A. T., Falk, S. P., and Weisblum, B. (2009) Phosphorylation of the RitR DNA-binding domain by a Ser-Thr phosphokinase: implications for global gene regulation in the streptococci. *Mol. Microbiol.* **71,** 382–390 CrossRef Medline
43. Chao, J. D., Papavinasasundaram, K. G., Zheng, X., Chávez-Steenbock, A., Wang, X., Lee, G. Q., and Av-Gay, Y. (2010) Convergence of Ser/Thr and two-component signaling to coordinate expression of the dormancy regulon in *Mycobacterium tuberculosis*. *J. Biol. Chem.* **285,** 29239–29246 CrossRef Medline
44. Agarwal, S., Agarwal, S., Pancholi, P., and Pancholi, V. (2011) Role of serine/threonine phosphatase (SP-STP) in *Streptococcus pyogenes* physiology and virulence. *J. Biol. Chem.* **286,** 41368–41380 CrossRef Medline
45. Agarwal, S., Agarwal, S., Pancholi, P., and Pancholi, V. (2012) Strain-specific regulatory role of eukaryote-like serine/threonine phosphatase in pneumococcal adherence. *Infect. Immun.* **80,** 1361–1372 CrossRef Medline
46. Fridman, M., Williams, G. D., Muzamal, U., Hunter, H., Siu, K. W., and Golemi-Kotra, D. (2013) Two unique phosphorylation-driven signaling pathways crosstalk in *Staphylococcus aureus* to modulate the cell-wall charge: Stk1/Stp1 meets GraSR. *Biochemistry* **52,** 7975–7986 CrossRef Medline
47. Canova, M. J., Baronian, G., Brelle, S., Cohen-Gonsaud, M., Bischoff, M., and Molle, V. (2014) A novel mode of regulation of the *Staphylococcus aureus* vancomycin-resistance-associated response regulator VraR mediated by Stk1 protein phosphorylation. *Biochem. Biophys. Res. Commun.* **447,** 165–171 CrossRef Medline
48. Horstmann, N., Saldaña, M., Sahasrabhojane, P., Yao, H., Su, X., Thompson, E., Koller, A., and Shelburne, S. A., 3rd. (2014) Dual-site phosphorylation of the control of virulence regulator impacts group a streptococcal global gene expression and pathogenesis. *PLoS Pathog.* **10,** e1004088 CrossRef Medline

49. Libby, E. A., Goss, L. A., and Dworkin, J. (2015) The eukaryotic-like Ser/Thr kinase PrkC regulates the essential WalRK two-component system in *Bacillus subtilis*. *PLoS Genet.* **11,** e1005275 CrossRef Medline
50. Bae, H. J., Lee, H. N., Baek, M. N., Park, E. J., Eom, C. Y., Ko, I. J., Kang, H. Y., and Oh, J. I. (2017) Inhibition of the DevSR two-component system by overexpression of *Mycobacterium tuberculosis* PknB in *Mycobacterium smegmatis*. *Mol. Cells* **40,** 632–642 Medline
51. Lee, H. N., Jung, K. E., Ko, I. J., Baik, H. S., and Oh, J. I. (2012) Protein-protein interactions between histidine kinases and response regulators of *Mycobacterium tuberculosis* H37Rv. *J. Microbiol.* **50,** 270–277 CrossRef Medline
52. Lee, H. N., Ji, C. J., Lee, H. H., Park, J., Seo, Y. S., Lee, J. W., and Oh, J. I. (2018) Roles of three FurA paralogs in the regulation of genes pertaining to peroxide defense in *Mycobacterium smegmatis* mc^2 155. *Mol. Microbiol.* **108,** 661–682 CrossRef Medline
53. Lee, H. N., Lee, N. O., Han, S. J., Ko, I. J., and Oh, J. I. (2014) Regulation of the *ahpC* gene encoding alkyl hydroperoxide reductase in *Mycobacterium smegmatis*. *PLoS ONE* **9,** e111680 CrossRef Medline
54. Baer, C. E., Iavarone, A. T., Alber, T., and Sassetti, C. M. (2014) Biochemical and spatial coincidence in the provisional Ser/Thr protein kinase interaction network of *Mycobacterium tuberculosis*. *J. Biol. Chem.* **289,** 20422–20433 CrossRef Medline
55. Gupta, M., Sajid, A., Arora, G., Tandon, V., and Singh, Y. (2009) Forkhead-associated domain-containing protein Rv0019c and polyketide-associated protein PapA5, from substrates of serine/threonine protein kinase PknB to interacting proteins of *Mycobacterium tuberculosis*. *J. Biol. Chem.* **284,** 34723–34734 CrossRef Medline
56. Molle, V., and Kremer, L. (2010) Division and cell envelope regulation by Ser/Thr phosphorylation: *Mycobacterium* shows the way. *Mol. Microbiol.* **75,** 1064–1077 CrossRef Medline
57. Sassetti, C. M., Boyd, D. H., and Rubin, E. J. (2003) Genes required for mycobacterial growth defined by high density mutagenesis. *Mol. Microbiol.* **48,** 77–84 CrossRef Medline
58. Manuse, S., Fleurie, A., Zucchini, L., Lesterlin, C., and Grangeasse, C. (2016) Role of eukaryotic-like serine/threonine kinases in bacterial cell division and morphogenesis. *FEMS Microbiol. Rev.* **40,** 41–56 CrossRef Medline
59. Richard-Greenblatt, M., and Av-Gay, Y. (2017) Epigenetic phosphorylation control of *Mycobacterium tuberculosis* infection and persistence. *Microbiol. Spectr.* **5** CrossRef Medline
60. Carette, X., Platig, J., Young, D. C., Helmel, M., Young, A. T., Wang, Z., Potluri, L. P., Moody, C. S., Zeng, J., Prisic, S., Paulson, J. N., Muntel, J., Madduri, A. V. R., Velarde, J., Mayfield, J. A., *et al.* (2018) Multisystem analysis of *Mycobacterium tuberculosis* reveals kinase-dependent remodeling of the pathogen-environment interface. *MBio* **9,** e02333-17 Medline
61. Young, T. A., Delagoutte, B., Endrizzi, J. A., Falick, A. M., and Alber, T. (2003) Structure of *Mycobacterium tuberculosis* PknB supports a universal activation mechanism for Ser/Thr protein kinases. *Nat. Struct. Biol.* **10,** 168–174 CrossRef Medline
62. Yeats, C., Finn, R. D., and Bateman, A. (2002) The PASTA domain: a β-lactam-binding domain. *Trends Biochem. Sci.* **27,** 438–440 CrossRef Medline
63. Ogawara, H. (2016) Distribution of PASTA domains in penicillin-binding proteins and serine/threonine kinases of *Actinobacteria*. *J. Antibiot.* **69,** 660–685 CrossRef Medline
64. Stock, J. B., Ninfa, A. J., and Stock, A. M. (1989) Protein phosphorylation and regulation of adaptive responses in bacteria. *Microbiol. Rev.* **53,** 450–490 Medline
65. Bourret, R. B., Hess, J. F., and Simon, M. I. (1990) Conserved aspartate residues and phosphorylation in signal transduction by the chemotaxis protein CheY. *Proc. Natl. Acad. Sci. U.S.A.* **87,** 41–45 CrossRef Medline
66. Lukat, G. S., Lee, B. H., Mottonen, J. M., Stock, A. M., and Stock, J. B. (1991) Roles of the highly conserved aspartate and lysine residues in the response regulator of bacterial chemotaxis. *J. Biol. Chem.* **266,** 8348–8354 Medline
67. Barthe, P., Mukamolova, G. V., Roumestand, C., and Cohen-Gonsaud, M. (2010) The structure of PknB extracellular PASTA domain from *Mycobacterium tuberculosis* suggests a ligand-dependent kinase activation. *Structure* **18,** 606–615 CrossRef Medline
68. Mir, M., Asong, J., Li, X., Cardot, J., Boons, G. J., and Husson, R. N. (2011) The extracytoplasmic domain of the *Mycobacterium tuberculosis* Ser/Thr kinase PknB binds specific muropeptides and is required for PknB localization. *PLoS Pathog.* **7,** e1002182 CrossRef Medline
69. Ortega, C., Liao, R., Anderson, L. N., Rustad, T., Ollodart, A. R., Wright, A. T., Sherman, D. R., and Grundner, C. (2014) *Mycobacterium tuberculosis* Ser/Thr protein kinase B mediates an oxygen-dependent replication switch. *PLoS Biol.* **12,** e1001746 CrossRef Medline
70. Sambrook, J., and Green, M. R. (2012) *Molecular Cloning: A Laboratory Manual*, 4th ed., Cold Spring Harbor Laboratory Press, Cold Spring Harbor, NY
71. Snapper, S. B., Melton, R. E., Mustafa, S., Kieser, T., and Jacobs, W. R., Jr. (1990) Isolation and characterization of efficient plasmid transformation mutants of *Mycobacterium smegmatis*. *Mol. Microbiol.* **4,** 1911–1919 CrossRef Medline
72. Oh, J. I., and Kaplan, S. (1999) The *cbb3* terminal oxidase of *Rhodobacter sphaeroides* 2.4.1: structural and functional implications for the regulation of spectral complex formation. *Biochemistry* **38,** 2688–2696 CrossRef Medline
73. Kim, M. J., Park, K. J., Ko, I. J., Kim, Y. M., and Oh, J. I. (2010) Different roles of DosS and DosT in the hypoxic adaptation of Mycobacteria. *J. Bacteriol.* **192,** 4868–4875 CrossRef Medline
74. Mouncey, N. J., and Kaplan, S. (1998) Redox-dependent gene regulation in *Rhodobacter sphaeroides* 2.4.1(T): effects on dimethyl sulfoxide reductase (dor) gene expression. *J. Bacteriol.* **180,** 5612–5618 Medline